CrossMark

Parametric analyses for synthetic jet control on separation and stall over rotor airfoil

Zhao Guoqing, Zhao Qijun *

National Key Laboratory of Rotorcraft Aeromechanics, Nanjing University of Aeronautics and Astronautics, Nanjing 210016, China

Abstract   Numerical simulations are performed to investigate the effects of synthetic jet control on separation and stall over rotor airfoils. The preconditioned and unsteady Reynolds-averaged Navier–Stokes equations coupled with a $k - \omega$ shear stream transport turbulence model are employed to accomplish the flowfield simulation of rotor airfoils under jet control. Additionally, a velocity boundary condition modeled by a sinusoidal function is developed to fulfill the perturbation effect of periodic jets. The validity of the present CFD procedure is evaluated by the simulated results of an isolated synthetic jet and the jet control case for airfoil NACA0015. Then, parametric analyses are conducted specifically for an OA213 rotor airfoil to investigate the effects of jet parameters (forcing frequency, jet location and momentum coefficient, jet direction, and distribution of jet arrays) on the control effect of the aerodynamic characteristics of a rotor airfoil. Preliminary results indicate that the efficiency of jet control can be improved with specific frequencies (the best lift-drag ratio at $F^+ = 2.0$) and jet angles (40° or 75°) when the jets are located near the separation point of the rotor airfoil. Furthermore, as a result of a suitable combination of jet arrays, the lift coefficient of the airfoil can be improved by nearly 100%, and the corresponding drag coefficient decreased by 26.5% in comparison with the single point control case.

1. Introduction

The retreating blades of a rotor are usually manipulated with large pitch angles. Therefore, flow separation and dynamic stall occur frequently during the forward flight of a helicopter.

The dynamic stall of retreating blades is one of the typical unsteady aerodynamic characteristics of a helicopter rotor, and it induces the loss of lift, the increase of drag and pitching moment of the rotor, which significantly impacts the aerodynamic performance of a helicopter, threatening the stability of the rotor and restricting the speed envelope of the helicopter. Strategies for delaying the flow separation and stall of the rotor (airfoil) and further extending the post stall envelope of the rotor (airfoil) have been an active topic in the field of helicopter technology for many years. The active flow control (AFC) method is a new approach in improving the aerodynamic characteristics of the rotor (airfoil), and is considered one of the innovative technologies for the next generation of

* Corresponding author. Tel.: +86 25 84893753.
  E-mail address: zhaoqijun@nuaa.edu.cn (Q. Zhao).

rotorcraft.[1] Furthermore, AFC has the potential to significantly improve the aerodynamic characteristics of airfoils without any deflecting control surfaces, which helps to retain a minimum radar cross section.

Recently, a novel method of AFC by using synthetic jet actuators has been experimentally demonstrated to be one of the most promising AFC methods, especially for rotary wing aircraft.[2] It is because the synthetic jet actuator generates a high-frequency jet from the flow with zero net mass injection. The synthetic jet actuator was manufactured by Smith and Glezer in 1994. A synthetic jet is created by driving one side of a cavity using a piston or piezoelectric diaphragm in a periodic manner, and the jet is synthesized by the interactions of counter rotating vortex pairs formed at the edge of an orifice.[3] The fluid driven out of the cavity forms a shear layer between the expelled fluid and the surrounding fluid. This layer of vorticity rolls up to form two parallel vortices in the case of a rectangular actuator. By the time the diaphragm begins to move away from the orifice to pull the fluid back into the cavity, the vortices have moved far away enough. Thus a train of vortex pairs are created by the actuator. Therefore, a synthetic jet requires no mass injection, but only electrical power. It is feasible for the flow control on the rotor and airfoil. Many experimental and numerical results demonstrate that a synthetic jet with appropriate combinations of parameters can reattach the separation flow over the rotor airfoils or delay its separation,[1,4–10] resulting in improving the aerodynamic characteristics of airfoils and delaying stall by enlarging the stall angle.

Seifert et al. carried out active flow control experiments on a NACA 0015 airfoil by placing a synthetic jet actuator at the leading edge,[11] and the results indicated that a jet placed just upstream of the separation location was effective on controlling the flow separation of an airfoil. In the aspect of numerical simulations for synthetic jet control, Donovan et al. used Reynolds-averaged Navier–Stokes (RANS) equations to investigate the effect of synthetic jet on the flowfield of an airfoil just according to the experiments,[12] and good agreements were obtained between the numerical results and the test data. The results give us the confidence that the RANS approach can be used to investigate the active flow control on rotor airfoils by using unsteady synthetic jets. Lorber et al. conducted numerical and experimental investigations on avoiding or delaying retreating blade stalls by a directed synthetic jet (DSJ) over helicopter rotor airfoil SC2110.[13] The results indicated that the DSJ was valuable on controlling the post and dynamic stall of a rotor retreating blade. Kim et al. numerically investigated the flow control using a synthetic jet to improve the aerodynamic performance of tiltrotor airfoils under various flight conditions,[14] and the calculated results revealed that the download could be efficiently reduced by using both the leading edge and trailing edge jets in the hovering flight mode.

Although the synthetic jet has a good potential in applications for active flow control on rotors and airfoils, there are some problems that have not been resolved.[15] The interactions of jet vortex pairs with low speed and viscous boundary layer are still not very clear yet, and the applications of the synthetic jet on a rotor airfoil still remain theoretical because of the large number of controlling parameters,[16] such as actuator location, forcing frequency, blowing magnitude and direction, etc. Additionally, there are some disagreements among different references. For example, He et al. pointed out that the

synthetic jet was not sensitive to the blowing directions,[16] while Hassan considered that the synthetic jet had the best performance when the jet angle was about 25°.[17] Furthermore, the numerical conclusions of Hassan preliminarily indicated that a jet array with two synthetic jet actuators could help improve the benefits of the enhancement of aerodynamic characteristics for rotor airfoils.[17] However, the research work only involved a two point AFC control with the actuators at a fixed location, while the control mechanism of synthetic jet arrays at various locations and with more than two actuators has not been taken into consideration.

This paper aims at obtaining in depth the effects of several parameters (especially jet angle and jet array) about the synthetic jet on the control efficiency of the aerodynamic characteristics of a rotor airfoil (measured by the increment or decrement rates of the aerodynamic forces of the rotor airfoil under control compared with the baseline case or a specified jet controlled case). Quite a number of numerical simulations have been conducted to investigate the effects of synthetic jet control on the separation and stall over rotor airfoils. To improve the accuracy of prediction on low speed flow induced by a synthetic jet with strong adverse pressure gradients and pressure-induced boundary layer separation, preconditioned RANS equations and a $k - \omega$ shear stream transport (SST) turbulent model are adopted to investigate the characteristics of the synthetic jet and the effectiveness of periodic jet control on the separation and post-stall for rotor airfoils. The feasibility and efficiency of this method are evaluated and demonstrated. Then, based on the present method, parametric analyses of synthetic jet control for rotor airfoil OA213 are carried out to study the control mechanism of the synthetic jet on the aerodynamic characteristics of the rotor airfoil, and some significant conclusions are obtained.

2. Numerical methods

2.1. Governing equations

Based on the CFD method developed by the author of this paper,[18] and to overcome the stiffness of the solution system and improve the computational efficiency when the local Mach number is low, flows around a rotor including unsteady perturbations induced by a synthetic jet are simulated by solving the unsteady preconditioned RANS equations. The preconditioned Navier–Stokes equations in a control volume Ω in the integral form by using pressure p, flow velocity u, v, and temperature T as parameters $W = [p, u, v, T]^{\mathrm{T}}$, can be written as

$$\Gamma \frac{\partial}{\partial t} \int W \mathrm{d}\Omega + \oint (\boldsymbol{F} - \boldsymbol{F}_{\mathrm{v}}) \cdot \boldsymbol{n} \mathrm{d}S = 0 \tag{1}$$

where $\boldsymbol{F}$, $\boldsymbol{F}_{\mathrm{v}}$ denote respectively the vectors of convective and viscous fluxes, $\boldsymbol{n}$ is the unit vector normal to surface element $\mathrm{d}S$, Γ the preconditioning matrix, and the Weiss–Smith matrix is employed in this paper.[19]

$$\Gamma = \begin{bmatrix} \Theta & 0 & 0 & \rho_T \\ \Theta u & \rho & 0 & \rho_T u \\ \Theta v & 0 & \rho & \rho_T v \\ \Theta H - 1 & \rho u & \rho v & \rho c_p + \rho_T H \end{bmatrix} \tag{2}$$

where H is the total enthalpy, c_p the isobaric specific heat capacity, ρ the local density of flow, ρ_T the partial derivative of the density to the temperature, parameter Θ is given by

$$\Theta = \frac{1}{U_r^2} - \frac{\rho_T}{\rho c_p}, \quad U_r = \min(\max(|V|, |V_\infty|), a) \qquad (3)$$

where V is the local velocity, V_∞ the velocity of free stream and a the speed of sound. The reference velocity, U_r, acts as a cut-off velocity above which the preconditioning method is turned off.

The dual-time iterative method is employed to simulate the periodic characteristics of a synthetic jet. The spatial discretization of Eq. (1) is accomplished by employing the Jameson finite volume scheme, and a modified artificial dissipation term according to the changed eigenvalues and flux of the preconditioned system has to be taken into account when implementing the spatial discretization scheme.

2.2. Turbulence model

The $K - \omega$ SST (two equations) turbulence model of Menter is employed to simulate the boundary layer flow on the rotor airfoil under jet control.[20,21] Written in time-dependent integral form for a control volume with a surface element dS, the SST turbulence model is

$$\frac{\partial}{\partial t} \int W_T d\Omega + \oint (F_T - F_{v,T}) \cdot n dS = \int Q_T dV \qquad (4)$$

The vector of conservative variables takes the form

$$W_T = \begin{bmatrix} \rho K \\ \rho \omega \end{bmatrix} \qquad (5)$$

where K is the turbulent kinetic energy, ω the turbulent dissipation rate, F_T, $F_{v,T}$ are vectors of convective and viscous fluxes respectively, Q_T is the source term. The turbulent eddy viscosity μ_T is obtained by

$$\mu_T = \frac{a_1 \rho K}{\max(a_1 \omega, f_2 \|\nabla \times v\|_2)}$$
$$f_2 = \tanh(\arg_2^2), \arg_2 = \max\left(\frac{2\sqrt{K}}{0.09\omega d}, \frac{500\mu_L}{\rho\omega d^2}\right) \qquad (6)$$

where $a_1 = 0.31$, μ_L is the laminar viscosity coefficient, d the minimum distance from the cell center to the surface of the airfoil.

2.3. Boundary conditions

A suction/blowing type velocity boundary condition was constructed to model the perturbation on the flow from the synthetic jet actuator. The non-dimensional velocity at the actuator surface is introduced by

$$v_{jet}(\xi, \eta = 0, t) = \sqrt{\frac{c}{2H_{jet}}} V_\infty \sqrt{2 < C_\mu >} \sin(2\pi F^+ t) f(\xi) n_{jet} \qquad (7)$$

where ξ denotes the streamwise direction, η the cross-stream direction, H_{jet} the effective jet width, V_∞ the velocity of free stream, $\langle C_\mu \rangle$ the oscillatory blowing coefficient, F^+ the non-dimensional jet frequency, t the physical time, $f(\xi)$ the spatial variation of jet over orifice, and n_{jet} is determined by the angle of the jet with the surface, as shown in Fig. 1, θ_{jet} is the jet angle between the jet vector and the surface of airfoil.
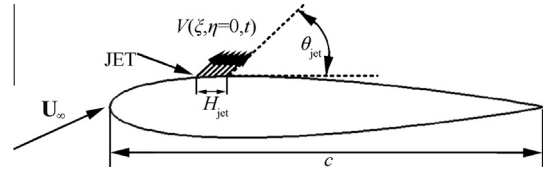

Fig. 1 Jet blowing/suction boundary condition on airfoil.

The spatial variation of the jet is specified by $f(\xi) = 1$. The non-dimensional frequency F^+ relates the frequency of the jet f to the convective frequency of the flow over the airfoil, so it is

$$F^+ = \frac{fc}{V_\infty} = \frac{\omega c}{2\pi V_\infty} \qquad (8)$$

The oscillation momentum coefficient $< C_\mu >$ determines the amplitude of the synthetic jet, and it is defined as

$$< C_\mu >= \frac{2H}{c}\left(\frac{u_{jet}^*}{V_\infty}\right)^2 \qquad (9)$$

with $< u_{jet}^* >$ being the root main square (RMS) velocity of the jet oscillation.

A modified boundary condition of the wall pressure at the synthetic jet orifice is established by considering the time-harmonic velocity perturbation, and the modified boundary condition becomes

$$\frac{\partial p}{\partial \eta} = -\rho \frac{\partial v}{\partial t} \cdot n_{jet} \qquad (10)$$

This condition stems from a consideration of the streamwise momentum equation, ignoring viscous effects. Eq. (10) shows that the pressure distribution over the jet orifice is determined by the percentage speed variation in the normal direction of the jet. For simplification, the pressure over the jet orifice is considered when calculating the aerodynamic forces of the rotor airfoil.

2.4. Grid generation

The grid around the rotor airfoil is generated by solving Poisson equations. In order to get more details of the synthetic jet, a clustering grid is adopted near the jet orifice. A C-type grid around NACA0012 is generated with a resolution of 356×70 in the chordwise and normal directions of the airfoil, respectively. There are 120 and 158 points on the lower and upper surfaces of the airfoil, respectively, 39 points on each of the wake cuts which extend from the airfoil's trailing edge to the outflow boundary of the farfield, and 11 points over the jet orifice. The grid is depicted in Fig. 2.

3. Validation and discussion

3.1. CFD method with preconditioning

Airfoil NACA0012 is taken as a numerical example with Mach number $Ma = 0.1$, angle of attack $\alpha = 3.59°$, and the multigrid method is used to accelerate the convergence process. Fig. 3 shows the convergence process of the simulation procedure and the pressure coefficient distribution of the airfoil with and without preconditioning. The Y-axis is the base 10 logarithm of the ratio for the current residual to the initial
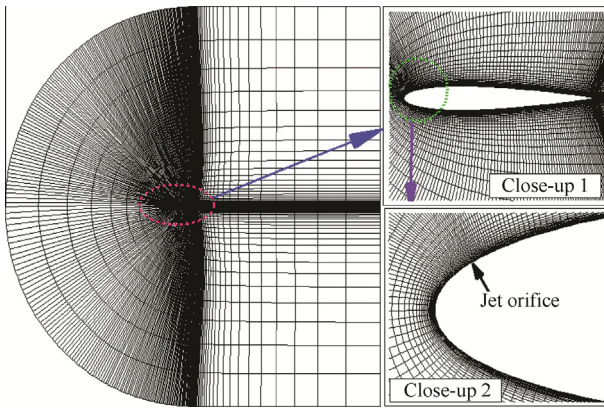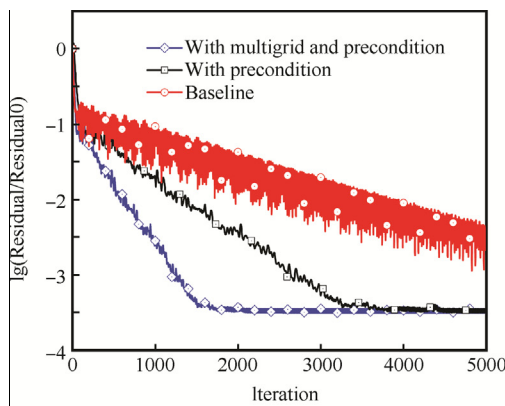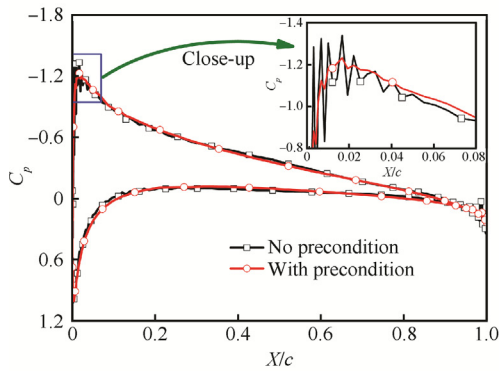
Fig. 2 Grid around rotor airfoil with clustering.

(a) Convergence process

(b) Pressure coefficient

Fig. 3 CFD convergence process and pressure coefficient distribution of airfoil.

residual. As can be seen, the preconditioning method can not only help accelerate the convergence, but also find the correct solution for this low-speed flow problem. In addition, the combination of the multi-grid and preconditioning methods shows significant improvement in the convergence rate of the present simulation method.

### 3.2. Simulations for an isolated jet

Firstly, the flowfield of an isolated synthetic jet is calculated. The width of the jet orifice H_{jet} is 0.5 mm, and the amplitude

of the velocity of the jet is 25 m/s with a perturbation frequency of 1000 Hz. The time history of the vorticity is characterized in Fig. 4. As can be seen, at half a period ($T/2$, where T is the size of jet period) of synthetic jet, pairs of counter-rotating vortices of the opposite sign form at the orifice of the jet and convect downstream. During the suction stroke ($T3/2$ in Fig. 4(b)), the vortex pair has convected a distance sufficiently away from the orifice, so that it is not affected by the intake flow. Thus the synthetic jet seems like a steady jet far away from the orifice.

Fig. 5 shows the time-averaged mean centerline velocity u_c with comparisons to the experimental data,[22] and the results are in good agreement. As can be seen, the streamwise velocity decreases along the centerline. Although the jet is formed by a strong time-harmonic motion, its farfield behavior is similar to a steady blowing jet.

Fig. 6 shows the mean cross-stream velocity profile over a range of distances from the orifice by comparing with the experimental data. The half-width of the jet, b, varies as a function of the distance from the wall, and it is determined as half the width of the jet profile which has half the value of the maximum velocity. At every cross-stream, the mean velocity profile all looks like a sinusoidal curve with a maximum value in the centerline, which is named self-similarity.

Then, a synthetic jet actuator is implemented at the leading edge of NACA0015 with the width being 0.14% of the chord length. The direction of the jet is normal to the surface of the airfoil. Fig. 7 shows the effect of $<C_\mu>$ on lift coefficient increment (ΔC_L) with $F^+ = 1.0$. As can be seen, ΔC_L increases as the oscillation momentum coefficient increases, and it is
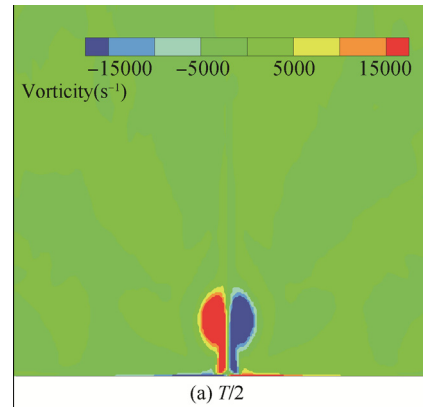
(a) $T/2$
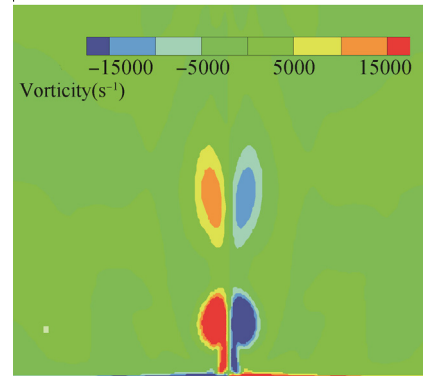
(b) $3T/2$

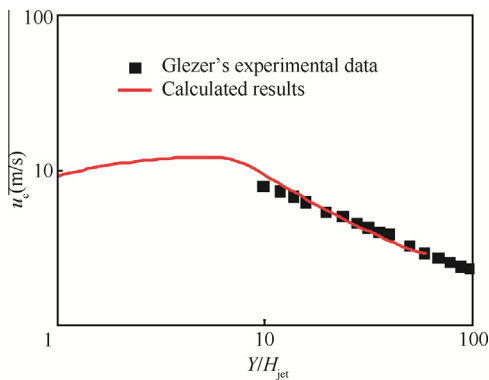**Fig. 4** Time evolution of the vorticity for an isolated synthetic jet.
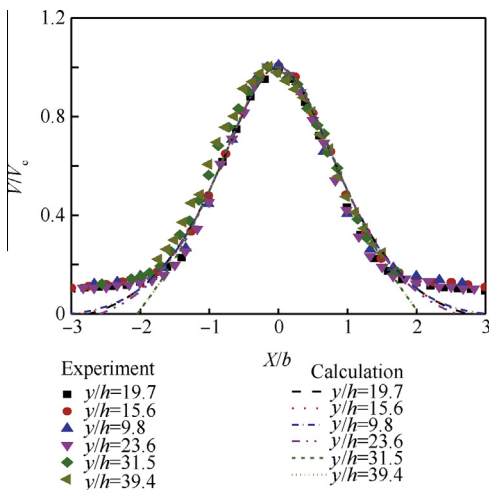
Fig. 5 Centerline streamwise velocity.

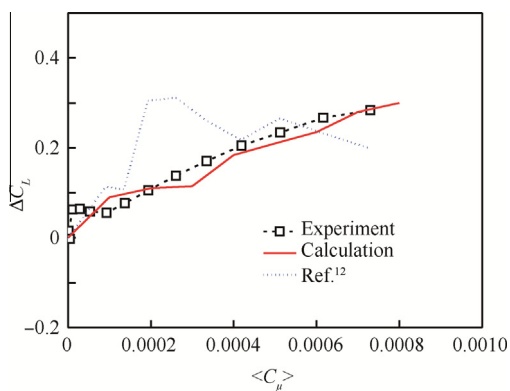**Fig. 6** Mean streamwise velocity profiles.

Fig. 7 Effect of blowing momentum on improvement of lift coefficient.

similar to the variation of the experimental data.[5] The numerical results are better than the results calculated by using incompressible RANS equations from Ref.[11].

3.3. Simulations for active flow control on NACA0012 airfoil

The investigations of synthetic jet control are performed on airfoil NACA0012 (its grid is shown in Fig. 2) with a jet actuator

centering at $1.5\%c$ and the width being $0.52\%c$ on the upper surface of the airfoil.

The simulations are conducted under the condition of a free stream Mach number being 0.4 (according to the condition of a retreating blade) and a post-stall angle of attack $\alpha = 22°$ and $Ma_\infty = 0.4$, $Re = 8.5 \times 10^6$. The oscillatory momentum and frequency of the synthetic jet are $<C_\mu> = 0.005$, $F^+ = 1.0$, respectively, and the jet angle $\theta_{jet} = 25°$.

Significant modifications of the flowfield are obtained as shown in Fig. 8, which demonstrates about 13% increment in lift value, 15% and 12% decrements in drag and pitching moment of the airfoil respectively in comparison to the baseline value. It indicates that the synthetic jet has the capability to improve the aerodynamic characteristics of rotor airfoils.

Fig. 9 further shows the streamlines over the airfoil in one jet control cycle at varied phases of ϕ. As shown in Fig. 9(a), flow separation occurs almost at the leading edge on the suction surface of NACA0012 airfoil. When jet control is applied, the flow reattaches near the leading edge, and the separated region is obviously less than that of the baseline case. The reattachment of the flow contributes to the increase in lift and reduction in drag of the airfoil. As can be seen from the figures, periodic vortex structures form at the location of the jet exportation, and then convect downstream, and the vortices lead to the stabilization of the boundary layer flow and decrease the local adverse pressure gradient. As a result, the separation of the flow on the suction surface of the airfoil is prevented or delayed.

In order to observe the jet control effects on the pressure of the airfoil, instantaneous pressure coefficient distributions on the surface of the airfoil controlled by a periodic synthetic jet are shown in Fig. 10. The presence of two coherent structures on the suction surface of the airfoil at every phase of the forcing is seen. The amplitude of the pressure oscillations on the suction surface decreases along the streamwise from the leading edge of the airfoil, and it is because the vortices formed at the location of the actuator travel together and interact with the separated flow.

The effects of the synthetic jet on the flowfield of airfoils depend on the two velocity components of the periodic jet. As shown in Fig. 11, the first and dominant one is vertical to the surface of the airfoil, and it can introduce a high-momentum outer fluid into the low-momentum inner boundary layer flow via the rotational motion of the vortex structures. The second one, which can energize the boundary layer flow by the additional momentum, is parallel to the streamwise flow. The two sources of vortices interact with the boundary layer and lead to the stability of the boundary layer flow.

4. Parametric analyses

Based on the calculated results of the synthetic jet control on a rotor airfoil, parametric analyses for synthetic jet control effect on the flowfield over rotor airfoil OA213 are performed. The control parameters of the jet include the magnitude of blowing momentum and angle, forcing frequency, jet location and distribution of jet arrays.

The jet actuators are placed on the upper surface of the airfoil at $5\%c$, $15\%c$, $30\%c$, $45\%c$ and $60\%c$, respectively, with
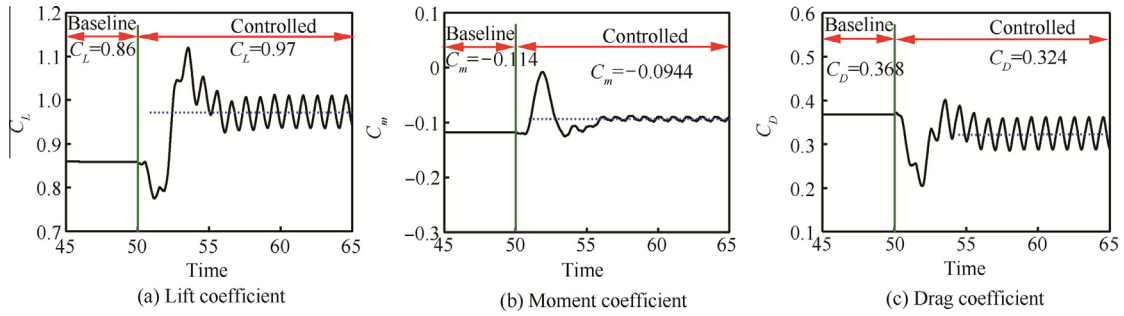
(a) Lift coefficient (b) Moment coefficient (c) Drag coefficient

Fig. 8   Predicted time history of aerodynamic forces of airfoil.

(a) Baseline   (b) $\phi=90°$ (c) $\phi=180°$

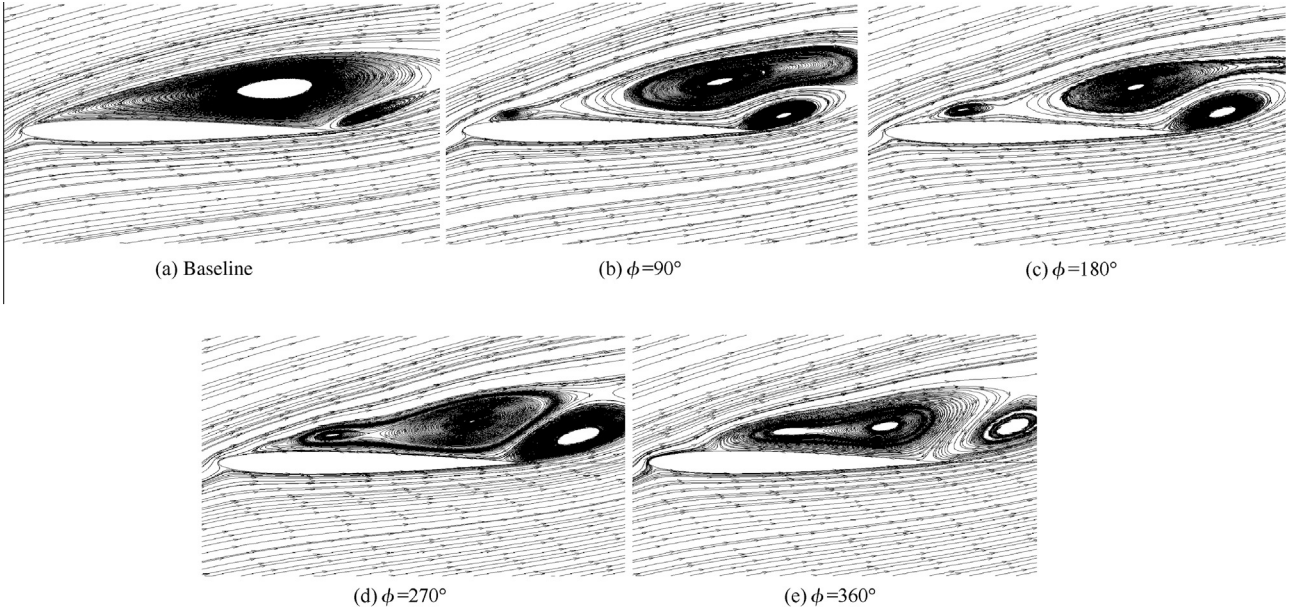(d) $\phi=270°$ (e) $\phi=360°$

Fig. 9   Close-up view of the streamlines around NACA0012 airfoil in one jet cycle.

the width of the jet orifice being $1.0\%c$, and the oscillatory momentum coefficients ranging from 0 to 0.01. The jet angles range from 0° to 90°. The free stream Mach number $Ma_\infty = 0.4$ and $Re = 8.5 \times 10^6$ (according to the condition of the retreating blade), and the angles of attack are 18°, 20° and 22°, respectively, under a post-stall condition.

4.1. Effects of oscillatory frequency
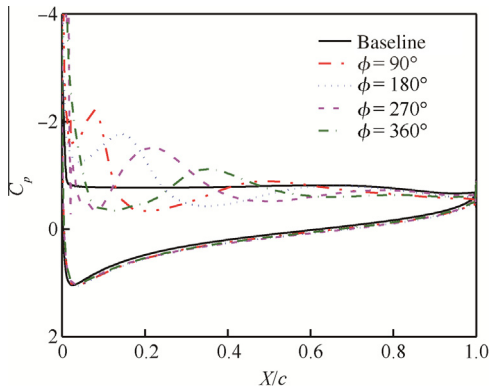
The jet is placed at $5\%c$ on the upper surface of the OA213 airfoil with the jet angle being 25°. Fig. 12 depicts the effects of non-dimensional jet frequencies on the lift, drag and moment coefficients of the airfoil. When $F^+ = 0.5$, the increment of the lift coefficient due to the perturbation of the jet reaches a maximum value. As the frequency increases, the effect of the jet on the mean lift decreases. The drag and moment coefficients of the airfoil have the largest improvement at the frequency of
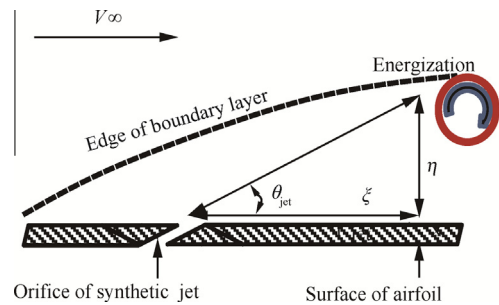

Fig. 10   Pressure coefficient distributions of airfoil in one jet cycle.

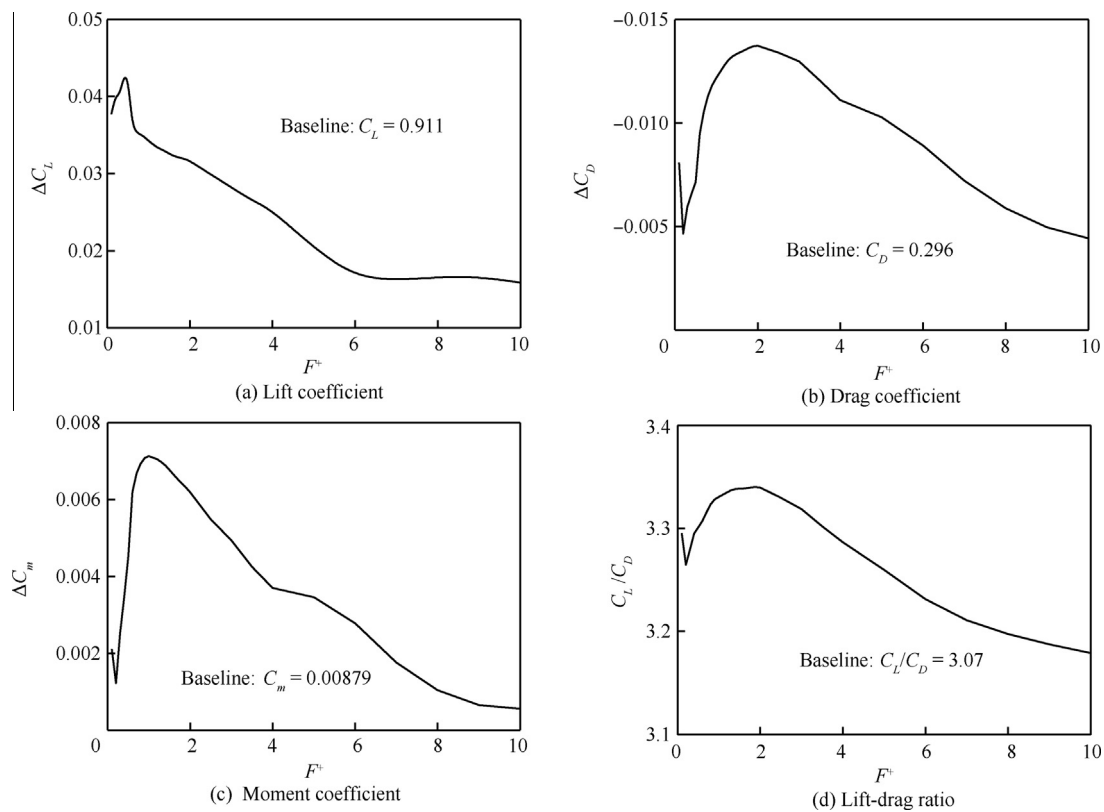**Fig. 11**   Schematic diagram of two components of the oscillatory jet.

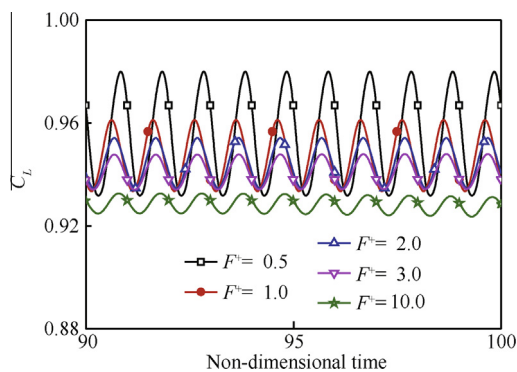**Fig. 12** Aerodynamic characteristics of airfoil under control vs jet frequencies.

Fig. 13 Convergence history of lift coefficients with different jet frequencies.
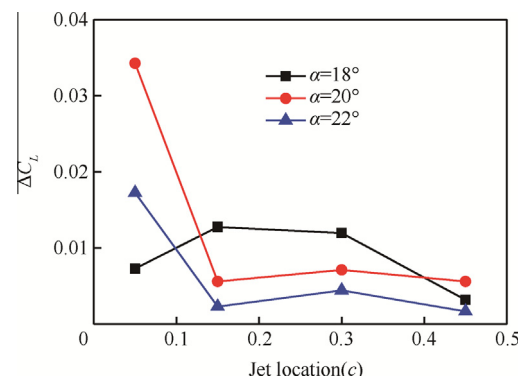

Fig. 14 Increment of lift coefficient of OA213 with different jet locations.

2.0 and 1.0, respectively, and the lift-drag ratio of the airfoil has a maximum value when F^+ is about 2.0. Furthermore, the control effects of the synthetic jet on the aerodynamic characteristics of the airfoil rapidly weaken when the forcing frequency is large than 2.0.

Fig. 13 shows the convergence process of the lift coefficients of the airfoil at different non-dimensional frequencies. As can be seen, the amplitude of the lift decreases as F^+ increases, and the maximum values of lift are more sensitive to the jet oscillation frequency.

4.2. Effects of jet location and angle of attack

Five jet slots, located at 5%c, 15%c, 30%c, 45%c and 60%c, respectively, with the same width (1.0%c) and under the same

jet control condition ($F^+ = 1.0$ and $<C_\mu> = 0.0007$), are compared in terms of their effects on the lift of the airfoil.

Fig. 14 shows the lift variations of controlled airfoil at different angles of attack with different jet locations. At the angle of attack of 18°, the jet control has a better improvement in the lift coefficient of the airfoil when the jet actuator is installed at 15%c from the leading edge. It is because flow separation occurs just near the position of 15%c on the upper surface of OA213 airfoil at the angle of attack of 18°; the control efficiencies of the synthetic jet decrease as the actuator is placed farther away from the separation point, as depicted in Fig. 15. As the angle of attack increases, the flow separation point moves towards the leading edge of the airfoil, and the jet at 5%c of the airfoil has a significant effect on the airfoil lift. The promoting effect due to the perturbation of the

synthetic jet decreases or even disappears when the jet actuator is located at the separated flow region.

4.3. Effect of blowing momentum

A variety of jet velocities are simulated to examine the effect of blowing magnitude on the efficiency of flow control. The oscillation momentum coefficients range from 0 to 0.01 (which denotes the maximum jet velocity is equal to the free stream velocity). The jet slot is located at $5\%c$ with the width of $1.0\%c$. The oscillatory frequency of the jet is $F^+ = 1.0$, and the angle of attack is $20°$.

The increments of lift, drag and moment coefficients of the airfoil due to the jet control at different jet blowing magnitudes are shown respectively in Fig. 16. As can be seen, with the increase of the forcing momentum, more energy can be transferred into the boundary layer with low momentum, and the controlling effect (such as lift increase and drag reduction et al.) enlarges.

Fig. 17 depicts the convergence procedure of the lift coefficients of the airfoil with three jet blowing magnitudes. As the forcing momentum increases, the lift of the airfoil increases and the amplitude increases also.

4.4. Effect of blowing direction (jet angle)

The effects of jet blowing direction are assessed by locating the angle between the jet and the surface of the airfoil (jet angle) from $0°$ to $90°$. Fig. 18 shows the magnitude of changed aerodynamic force coefficients versus jet angle θ_{jet} with different
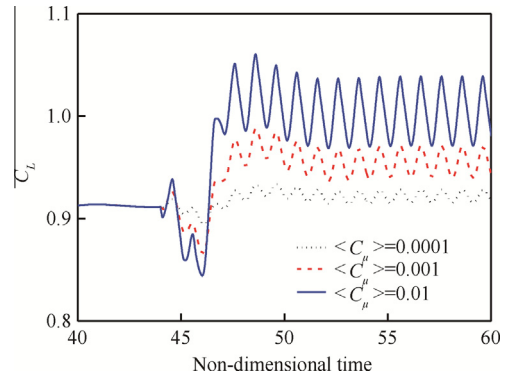
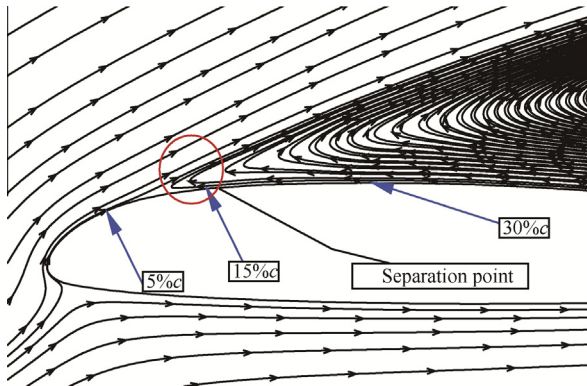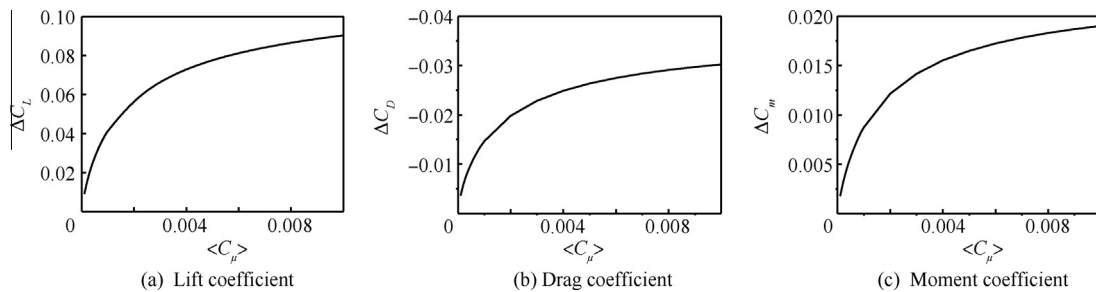**Fig. 17** Lift coefficients of airfoil vs time at different forcing magnitudes.

oscillatory momentum coefficients. When the jet convects tangentially downstream, the jet control is almost ineffective. It is because the small jet angle causes the component of the blowing momentum vertical to the surface of the airfoil to be insufficient to introduce high-momentum fluid into the low-momentum boundary layer flow as shown in Fig. 11. As the angle increases up to $75°$, the mean lift of the airfoil increases to a stable value when $<C_\mu> = 0.0007$, while there are maximum benefits at θ_{jet} of about $40°$ and a corresponding $<C_\mu> = 0.0007$.

The numerical results indicate that the jet with low momentum has the best control effect on the aerodynamic force of an airfoil when the jet angle is large enough, while the jet with high momentum is most efficient with a much smaller jet angle. Other than this, there are some differences between the present results and the conclusions of He et al.[15] and Hassan.[16] Although the investigations are conducted with different airfoils under different flow conditions, the significant cause of the disagreements may be due to the magnitude of blowing momentum of the synthetic jet. When the velocity of the jet is low, it requires a large angle to maintain the momentum component vertical to the surface of the airfoil, which enables the synthetic jet with enough momentum to energize the boundary layer. On the other hand, the synthetic jet with sufficient momentum has the highest efficiency with a smaller jet angle; if the jet angle is too large, the interactions between the periodic jet and the boundary layer weaken the more favorable control effect on the aerodynamic characteristics of the airfoil.

Fig. 19 depicts the convergence history of the lift coefficients of the airfoil with different jet angles. The results indicate that a large jet angle can induce a large lift coefficient

Fig. 15 Streamlines of baseline case around OA213 airfoil at $\alpha = 18°$.

(a) Lift coefficient

(b) Drag coefficient

(c) Moment coefficient

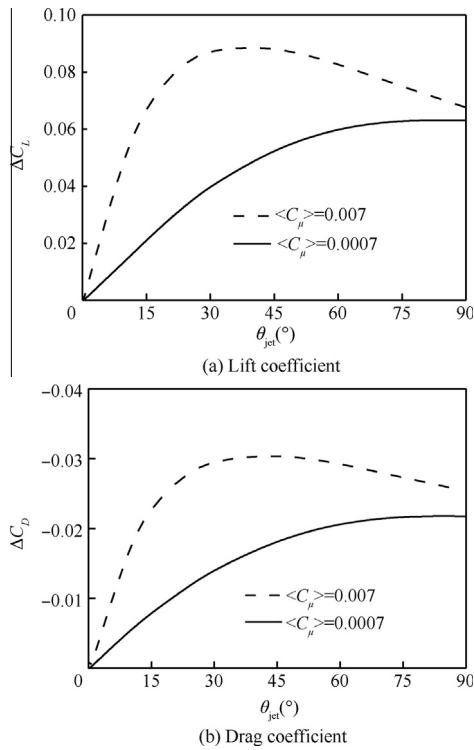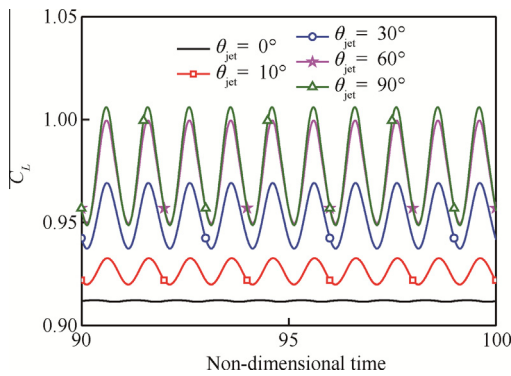**Fig. 16** Force coefficients of airfoil under jet control at different forcing magnitudes.

Fig. 18 Magnitude of changed aerodynamic force coefficients vs jet angle.

Fig. 19 Convergence history of lift coefficients of the airfoil with different jet angles.

and a large amplitude of the time-varying oscillatory lift coefficient of the airfoil.

4.5. Effect of jet arrays

The control effects of different jet arrays on the characteristics of OA213 airfoil are investigated. Five jet actuators are installed at 5%c, 15%c, 30%c, 45%c and 60%c, respectively, with the same width (1.0%c). The numbers and the location of the jets are shown in Fig. 20, and the combinations of the jet actuator arrays are shown in Table 1. As a supplement, the effects of jet arrays are investigated by setting jet actuators with the same phases.

Fig. 21 shows the variations of lift and drag coefficients of the airfoil under different jet array combinations, and all the

jet actuators have the same magnitude of blowing momentum (0.0007) and jet angle (25°) (named as Case 1). Compared to a single jet actuator, the combinations of jet arrays can lead to the improvement of aerodynamic characteristics of the airfoil, such as a maximum increment of the lift coefficient of about 26% and a maximum decrement of drag coefficient of about 13%, respectively. The numerical results indicate that by prudentially choosing the combinations of jet arrays, the separation of flow and stall over a rotor airfoil can be prevented or delayed. At the same time, the simulated result shows that various combinations of jet arrays can provide different improvements of the aerodynamic force of the airfoil, and it also indicates that jet arrays with more jet actuators may unnecessarily in order to achieve a better performance of the airfoil.

According to the conclusions above, a set of jet parameters is combined to investigate the control effect of synthetic jet arrays on the lift and drag characteristics of an airfoil. The numbers of different combinations of jet arrays are the same
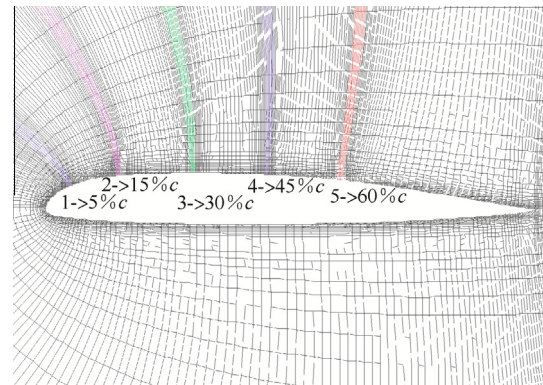
Fig. 20 Locations of different jet actuators at the upper surface of airfoil.

Table 1 Number of combinations of jet arrays.

| Number of arrays	0	1	2	3	4	5	6	7
Combination of jet actuators	1	1–2	1–3	1–4	1–5	1–2–3	1–2–4	1–2–5
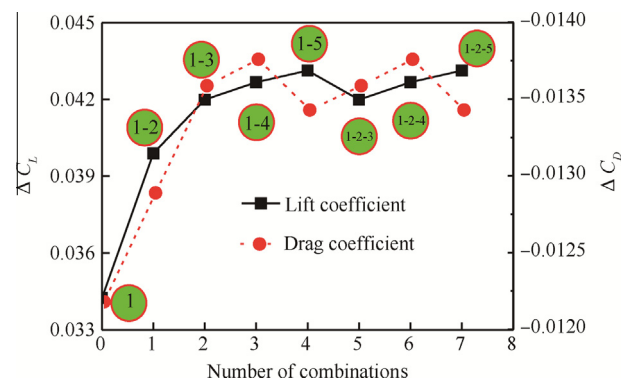
Fig. 21 Variations of lift and drag coefficients with different combinations of jet arrays.

as Table 1, and the jet parameters of each jet actuator are presented in Table 2 (Case 2) with the blowing momentum ten times the value of Case 1 and various jet angles from 40° to 75°. Fig. 22 predicts the magnitude of the variations of lift, drag coefficients and lift-drag ratio of the airfoil. As can be seen in Fig. 22(a), the control efficiency of the synthetic jet is improved by a maximum magnitude of about 100% in lift coefficient and about 26.5% in drag coefficient of the airfoil, respectively, as compared to the control example using only one synthetic jet.

The numerical results of the two cases indicate that the synthetic jet control is more effective on lift coefficient than drag coefficient. Moreover, a comparison of the lift-drag ratio is performed in Fig. 22(b), and the magnitudes of the ratio show that synthetic jet control technology can obviously improve the control efficiency on the aerodynamic characteristics of a rotor airfoil by understanding the mechanism of synthetic jet control and further employing an effective combination of jet parameters including jet arrays.

Table 2 Parameters of each jet actuator (Case 2).

Number of jet actuators	Oscillatory frequency F^+	Jet angle (°)	Blowing momentum
1	2.0	40	0.007
2	2.0	45	0.007
3	2.0	55	0.007
4	2.0	65	0.007
5	2.0	75	0.007
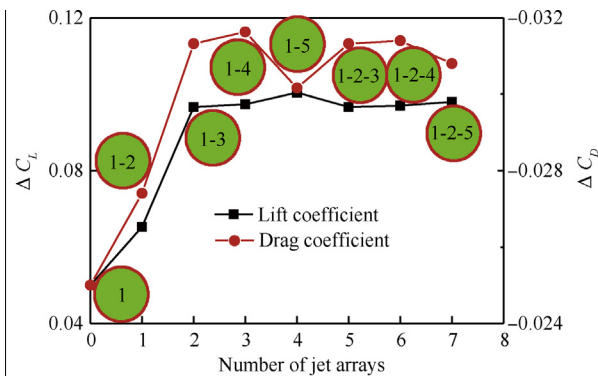
(a) Variations of lift and drag coefficients
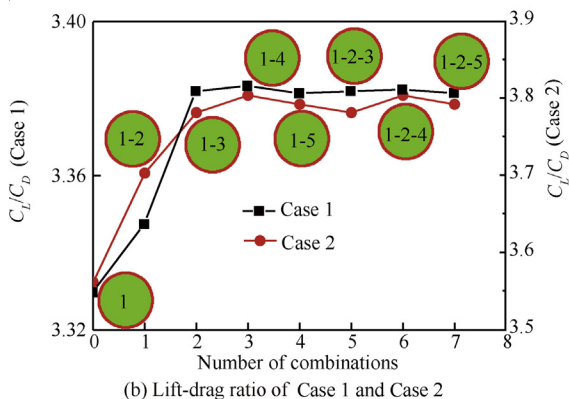
(b) Lift-drag ratio of Case 1 and Case 2

Fig. 22 Variations of aerodynamic characteristics with different combinations of jet arrays.

5. Conclusions

Numerical simulations are carried out to investigate the control effects of synthetic jets on delaying flow separation and improving the aerodynamic characteristics of a rotor airfoil under post-stall states. Based upon the established numerical method, parametric analyses are conducted specifically to investigate the effects of jet parameters on the aerodynamic characteristics of rotor airfoil OA213 under a typical operation condition for retreating blades at $Ma_\infty = 0.4$ and $Re = 8.5 \times 10^6$.

(1) The numerical method utilizing the RANS equations and blowing/suction and pressure boundary condition of a synthetic jet can effectively simulate the characteristics of the synthetic jet and the aerodynamic characteristics of the rotor airfoil w/o synthetic jet control.

(2) The farfield behavior of an isolated synthetic jet is similar to a steady blowing jet, and the cross-stream velocity profile shows a self-similar characteristic. The interactions of vortex pairs introduced by the synthetic jet and embedding flow have the potential to lead to the stabilization of the boundary layer, thus preventing or delaying the separation of the flow on the suction surface of the airfoil.

(3) Synthetic jet has the best performance when it is mounted near the flow separation point on the surface of the rotor airfoil. The aerodynamic forces of the rotor airfoil have different performances with the variation of jet frequency: a maximum lift coefficient of the airfoil appears when the jet frequency $F^+ = 0.5$, and drag and moment coefficients have minimum values with $F^+ = 2.0, 1.0$, respectively. Synthetic blowing momentum plays a very important role in the active flow control on the aerodynamic characteristics of the rotor airfoil, and a large magnitude of blowing momentum can lead to a significant improvement of the aerodynamic forces of the rotor airfoil.

(4) With varied blowing momentums, the best control effects of the synthetic jet on the aerodynamic characteristics of the rotor airfoil can be obtained at different jet angles. When the blowing momentum is low, the jet has the best control effect on the aerodynamic forces of the airfoil when the jet angle is large enough (even up to 90°). On the other hand, a synthetic jet with a smaller jet angle is more effective when it has higher blowing momentum.

(5) Compared to a single jet actuator, reasonable combinations of jet arrays with the same phases can more obviously improve the jet control efficiency on preventing or delaying the separation of flow and stall over a rotor airfoil. For example, the lift and drag coefficients can be improved by a maximum of about 100% and 26.5%, respectively, when the stall of the rotor airfoil is controlled by a combination of jet arrays.

To further obtain the best combination of jet parameters and jet arrays in improving the aerodynamic performances of rotor airfoils, the effect of phase relationships among jet arrays on control efficiency and the optimization method should be studied in future for the investigation of stall and separation control of rotor (airfoil) by using synthetic jets.

Acknowledgement

References

1. Melton LP, Hannon J, Yao CS, Harris J. Active flow control at low Reynolds numbers on a NACA 0015 airfoil. Report No.: AIAA-2008-6407, 2008.
2. Hassan AA, JanakiRam RD. Effects of zero-mass synthetic jets on the aerodynamics of the NACA-0012 airfoil. Report No.: AIAA-1997-2326, 1997.
3. Smith BL, Glezer A. Vector and small-scale motions effected in free shear flows using synthetic jet actuators. Report No.: AIAA-1997-0213, 1997.
4. Seifert A, Darabi A, Wygnanski I. Delay of airfoil stall by periodic excitation. J Aircr 1996;33(4):691–8.
5. Hassan AA. Numerical simulations and potential applications of zero-mass jets for enhanced rotorcraft aerodynamic performance. Report No.: AIAA-1998-0211, 1998.
6. Tabatabaeian S, Mirzaei M, Sadighzadeh A, Damideh V, Shadaram A. Experimental investigation of the effects of various plasma actuator configurations on lift and drag coefficients of a circular cylinder including the effects of electrodes. Chin J Aeronaut 2012;25(3):311–24.
7. Traub LW, Miller A, Rediniotis O. Effects of synthetic jet actuation on a ramping NACA 0015 airfoil. J Aircr 2004;41(5):1153–62.
8. Nagib H, Greenblatt D, Kiedaisch J. Effective flow control for rotorcraft applications at flight Mach number. Report No.: AIAA-2001-2974, 2001.
9. Han ZH, Zhang KS, Song WP, Qiao ZD. Optimization of active flow control over an airfoil using a surrogate-management framework. J Aircr 2010;47(2):603–12.
10. Xu XP, Zhu XP, Zhou Z, Fan RJ. Application of active flow control technique for gust load alleviation. Chin J Aeronaut 2011;24(4):410–6.
11. Seifert A, Pack LG. Oscillatory excitation of unsteady compressible flows over airfoils at flight Reynolds numbers. Report No.: AIAA-1999-0925, 1999.
12. Donovan JF, Kral LD, Cary AW. Active flow control applied to an airfoil. Report No.: AIAA-1998-16119, 1998.
13. Lorber P, McCormick D, Anderson T, Wake B, MacMartin D, Pollack M, et al. Rotorcraft retreating blade stall control. Report No.: AIAA-2000-2475, 2000.
14. Kim M, Kim S, Kim W, Kim C, Kim Y. Flow control of tiltrotor unmanned-aerial-vehicle airfoils using synthetic jets. J Aircr 2011;48(3):1045–56.
15. Kral LD, Donovan JF, Cain AB, Smith TD. Numerical simulation of synthetic jet actuator. Report No.: AIAA-1997-1824, 1997.
16. He YY, Cary AW, Peters DA. Parametric and dynamic modeling for synthetic jet control of a post-stall airfoil. Report No.: AIAA-2001-733, 2001.
17. Hassan AA. A two-point active flow control strategy for improved airfoil stall/post stall aerodynamics. Report No.: AIAA-2006-99, 2006.
18. Zhao QJ, Xu GH, Zhao JG. New hybrid method for predicting the flowfield of helicopter in hover and forward flight. J Aircr 2006;43(2):372–80.
19. Weiss JM, Maruszewski JP, Smith WA. Implicit solution of preconditioned Navier–Stokes equations using algebraic multigrid. AIAA J 1999;37(1):29–36.
20. Menter FR. Two-equation eddy-viscosity turbulence models for engineering applications. AIAA J 1994;32(8):1598–605.
21. Tu GH, Deng XG, Mao ML. Flow control of tiltrotor unmanned-aerial-vehicle airfoils using synthetic jets. Chin J Aeronaut 2012;25(1):25–32.
22. Smith BL, Glezer A. The formation and evolution of synthetic jets. Phys Fluids 1998;10(9):2281–97.

Zhao Guoqing is a Ph.D. candidate in aircraft design at Nanjing University of Aeronautics and Astronautics, and his research interests are active flow control of rotors, helicopter CFD and helicopter aerodynamics.

Zhao Qijun is a professor and Ph.D. supervisor in the College of Aerospace Engineering at Nanjing University of Aeronautics and Astronautics, where he received his Ph.D. in aircraft design. His main research interests are helicopter CFD, helicopter aerodynamics, aerodynamic shape design of rotor blades, active flow control of rotors, and rotor aeroacoustics.